Received: 30 June 2023 | Revised: 26 September 2023 | Accepted: 2 October 2023

DOI: 10.1002/dvdy.670

Developmental Dynamics WILEY

PHENOTYPE REPORT

Kdm7a expression is spatiotemporally regulated in developing *Xenopus laevis* embryos, and its overexpression influences late retinal development

Davide Martini | Matteo Digregorio | Ilaria Anna Pia Voto | Giuseppe Morabito | Andrea Degl'Innocenti | Guido Giudetti | Martina Giannaccini | Massimiliano Andreazzoli

Department of Biology, University of Pisa, Pisa, Italy

Correspondence
Massimiliano Andreazzoli, Department of Biology, University of Pisa, SS12 Abetone e Brennero, 4, I-56127 Pisa, Italy.
Email: massimiliano.andreazzoli@unipi.it

Present addresses
Andrea Degl'Innocenti, Department of Medical Biotechnologies, University of Siena, Siena, Italy; Smart Bio-Interfaces, Italian Institute of Technology, Pontedera, Italy; and Guido Giudetti, European Research Executive Agency, Bruxelles, Belgium.

Funding information
University of Pisa

Abstract

Background: Post-translational histone modifications are among the most common epigenetic modifications that orchestrate gene expression, playing a pivotal role during embryonic development and in various pathological conditions. Among histone lysine demethylases, KDM7A, also known as KIAA1718 or JHDM1D, catalyzes the demethylation of H3K9me1/2 and H3K27me1/2, leading to transcriptional regulation. Previous data suggest that KDM7A plays a central role in several biological processes, including cell proliferation, commitment, differentiation, apoptosis, and maintenance. However, information on the expression pattern of *KDM7A* in whole organisms is limited, and its functional role is still unclear.

Results: In *Xenopus* development, *kdm7a* is expressed early, undergoing spatiotemporal regulation in various organs and tissues, including the central nervous system and the eye. Focusing on retinal development, we found that *kdm7a* overexpression does not affect the expression of genes critically involved in early neural development and eye-field specification, whereas unbalances the distribution of neural cell subtypes in the mature retina by disfavoring the development of ganglion cells while promoting that of horizontal cells.

Conclusions: *Kdm7a* is dynamically expressed during embryonic development, and its overexpression influences late retinal development, suggesting a potential involvement in the molecular machinery regulating the spatiotemporally ordered generation of retinal neuronal subtypes.

KEYWORDS

demethylase, epigenetics, expression, eye, histone, neuron

1 | INTRODUCTION

Epigenetics consists in a series of complex and dynamically reversible chemical modifications within DNA and histone proteins that lead to the remodeling of heterochromatin to euchromatin or vice versa, thus regulating the accessibility of transcription factors and RNA polymerase II to target *loci* and, ultimately, modulating gene transcription.[1] Epigenetics is critically involved in the regulation of several cellular processes, and its importance during development has been highlighted in a wide number of works.[1,2] Several results show that alterations of the epigenetic machinery contribute to different pathologies, and a growing amount of evidence indicates that the epigenetic state of various tissues represents an important diagnostic and prognostic biomarker. Indeed, chromatin regulation is increasingly considered an important target for therapeutic strategies, aimed at counteracting specific diseases. In this respect, some epigenetic-based drugs are undergoing clinical trials, and others have already been introduced into clinical use.[1,3]

Methylation of arginine (R) or lysine (K) residues on histone protruding N-terminal tails is among the most common post-translational histone modifications. In particular, K residues can be mono- (me1), di- (me2), or tri- (me3) methylated, with the location and the level of histone K-methylation determining either the activation or the repression of gene transcription. For instance, histone 3 (H3) K4 methylation is generally reported in promoter regions of actively transcribed genes, whereas high methylation states of H3K9 and H3K27 usually correlate with transcriptional silencing. Histone K-methyltransferase (KMTs) are the enzymes that carry out methyl group addition to K residues, while histone K-demethylases (KDMs) catalyze the removal of methyl groups.[2]

Among KDMs, the Jumonji C (JmjC) domain-containing enzymes remove methyl groups from K residues by hydroxylation, in an Fe(II) and α-ketoglutarate-dependent reaction. KDM7A, also known as KIAA1718 or JHDM1D, harbors two domains in its N-terminal half: a plant homeodomain (PHD), with a Zn-finger motif that binds to H3K4me3, and a JmjC domain, catalyzing the demethylation of H3K9me1/2 and H3K27me1/2, although the demethylation of monomethylated H3K9 and H3K27 histones has been questioned by some authors.[4–8] Various works indicate that KDM7A is involved in a plethora of biological processes, including—for instance—cell-fate determination, neural differentiation/development,[4–6,8–10] stem-cell[11] or progenitor-cell state maintenance,[10] and apoptosis.[11] KDM7A is evolutionarily conserved from *Caenorhabditis elegans* to humans, and some evidence indicates its involvement in the regulation of gene transcription in several tissues, including the nervous system.[6,9] The role and mechanisms underlying KDM7A-mediated transcriptional regulation, however, are far from being elucidated. Additionally, data on KDM7A expression pattern in whole organisms are limited, although this type of information could provide clues on its functional role.[5,6,9,12] It is known that functionally and morphologically distinct types of cells generate and differentiate from common proliferative progenitors during central nervous system (CNS) development. In this respect, researchers often focused on the vertebrate retina as a model of CNS development and functionality. Indeed, just like other CNS regions, retinal cells are organized in ordered layers (outer nuclear layer, ONL; inner nuclear layer, INL; and ganglion cells layer, GCL) based on their specialized function, to effectively capture and integrate sensory information. Additionally, several cellular processes and molecular pathways involved in CNS formation play a central role in retinal development as well.[13] With conserved modalities across vertebrates, retinal progenitor cells (RPCs) are initially specified at early neurula stage in the eye field, the anteriormost region of the neuroectoderm. Successively, RPCs proliferate, concurrently losing their developmental potential and progressively differentiating—in a finely regulated spatiotemporal order—to generate the different cell populations, guided by a complex and synchronized regulation of gene expression. In this way, five retinal neuronal cell subsets, namely ganglion cells, cone photoreceptors, horizontal cells, amacrine cells, rod photoreceptors, and the Müller glia cells, are generated in partially overlapping waves.[13,14] Interestingly, several studies in various experimental models, including *Xenopus*, showed that epigenetic mechanisms, including histone K-methylation and demethylation, are pivotal in retinal cell-fate determination, maturation, survival, and more generally in eye development.[15–23] Still, data on the role of KDM7A during retina formation are scarce, although a previous work in developing *Xenopus laevis* embryos showed that *kdm7a* is among the genes regulated by Rax/Rx1, a well-known paired-like homeodomain transcription factor critical for vertebrate retina specification and morphogenesis, suggesting a potential involvement of Kdm7a in retinal development.[12]

Here, we provide a detailed spatiotemporal expression pattern of *kdm7a* during *Xenopus laevis* embryonic development, and find that its overexpression specifically affects late retinal development.

2 | RESULTS AND DISCUSSION

2.1 | Temporal expression of *kdm7a*

Our real-time reverse transcription-polymerase chain reaction (RT-qPCR) analysis (Figure 1) shows that *kdm7a*

transcripts are already detectable at eight-cell stage (St. 4) before midblastula transition (St. 8),[24] suggesting a potential role for Kdm7a during the earliest phases of development, in line with previous works on KMTs and other KDMs.[2,17,19,20] Additionally, even though studies in zebrafish and chick embryos did not specifically assess the presence of a maternal transcript for the respective *kdm7a* orthologues,[6,9] modulation of *KDM7A* mRNA levels in developing porcine and bovine embryos was reported around embryonic genome activation transition.[25]

As *Xenopus* development proceeds, *kdm7a* expression is maintained at St. 7, only to decrease around late gastrula stage (St. 11). During the considered subsequent stages of development, expression levels remain almost unchanged, with only a slight increasing trend. Evidence of a dynamic temporal regulation of *kdm7a* expression in development is reported in various experimental models, such as mouse,[5,26] zebrafish,[6] pig,[25] and cattle.[25]

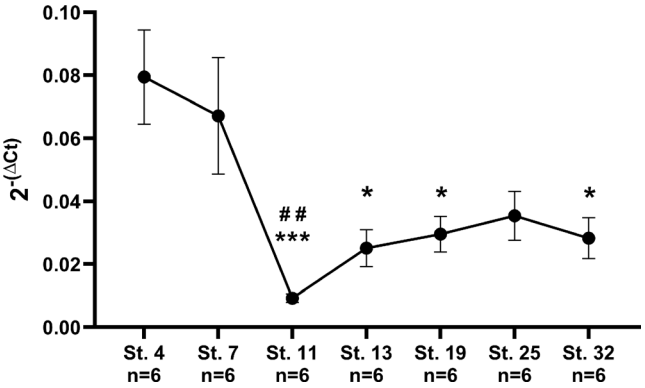

FIGURE 1 Real-time reverse transcription-polymerase chain reaction (RT-qPCR) analysis of *kdm7a* expression in developing embryos. cDNAs were synthesized from embryos and larvae at the indicated developmental stages (St.: stage), and amplified by RT-qPCR using primers specific for *kdm7a*, as well as for *sub1.S*, *slc35b1.L*, and *ppp1ca.L*, used for normalization. *n*: number of samples. Asterisks (*) indicate statistical comparisons between each stage and stage 4 (St. 4); hash marks (#) indicate statistical comparisons between each stage and stage 7 (St. 7). Data are expressed as mean ± standard error of the mean. ANOVA followed by Tukey post-hoc test: $^{*}p < .05$; $^{***}p < .001$; $^{\#\#}p < .01$.

2.2 | Spatial expression pattern of *kdm7a*

We analyzed the spatial expression pattern of *kdm7a* by performing in situ hybridization (ISH) throughout development. During the earliest blastula stages, before midblastula, maternal *kdm7a* transcripts mainly localize in the animal hemisphere (St. 4 and 7, Figure 2A,B/B′,

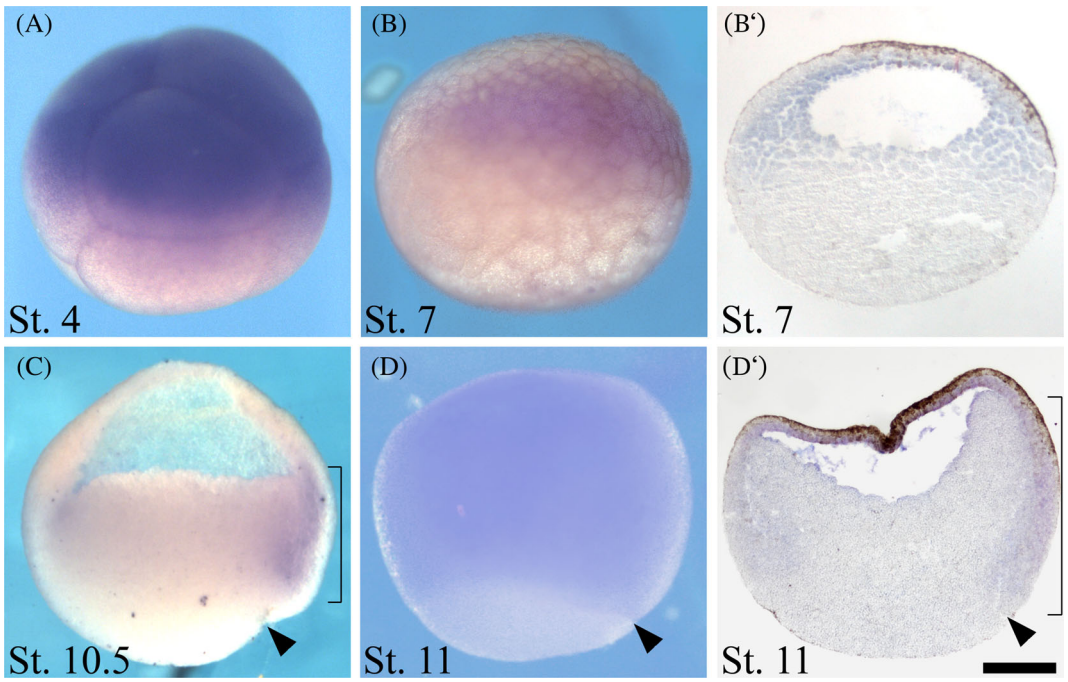

FIGURE 2 In situ hybridization analysis of *kdm7a* during segmentation and gastrulation. Embryo developmental stages are indicated at the bottom-left corner of each panel (St.: stage). Lateral view of St. 4, 7, 10.5, 11 embryos (A, B/B′, C, D/D′, respectively). Whole-mount embryos (A, B, D), emi-gastrulae (C), or sagittal sections from whole-mount-stained embryos (B′, D′) are represented in the panel. Animal pole to the top, vegetal pole to the bottom. Black arrowheads point to the dorsal lip of the blastopore; brackets indicate the dorsal involuting mesoderm. An average of 25 embryos was used for each of the analyzed stages. Scale bar 150 μm.

respectively). At early gastrula stage (St. 10.5, Figure 2C), *kdm7a* mRNA signal is present in the presumptive mesoderm, with particular intensity in the dorsal side. This pattern is maintained also at St. 11, when *kdm7a* is found in the dorsal and in ventral involuting mesoderm (Figure 2D,D′).

At early neurula stage of *Xenopus laevis* (St.13, Figure 3A,A′), a weak *kdm7a* signal is localized in both the anterior and dorsal regions of the neural plate, and in the dorsal paraxial mesoderm. In agreement with our observations, *KDM7A* expression at both mRNA and protein level was reported in the neural plate of developing chick embryos.[9] At St. 16 (Figure 3B,B′), the expression pattern of *kdm7a* becomes more demarcated in the most anterior region of the neural plate and in the neural crest territory, while an additional signal is observed in the region of cardiac progenitors, ventrally to the unlabeled cement gland primordium. Subsequently, after neural tube closure (St. 19, Figure 3C,C′), *kdm7a* mRNA is clearly detected in the neural tube, in optic vesicles, and in migrating neural crest cells.

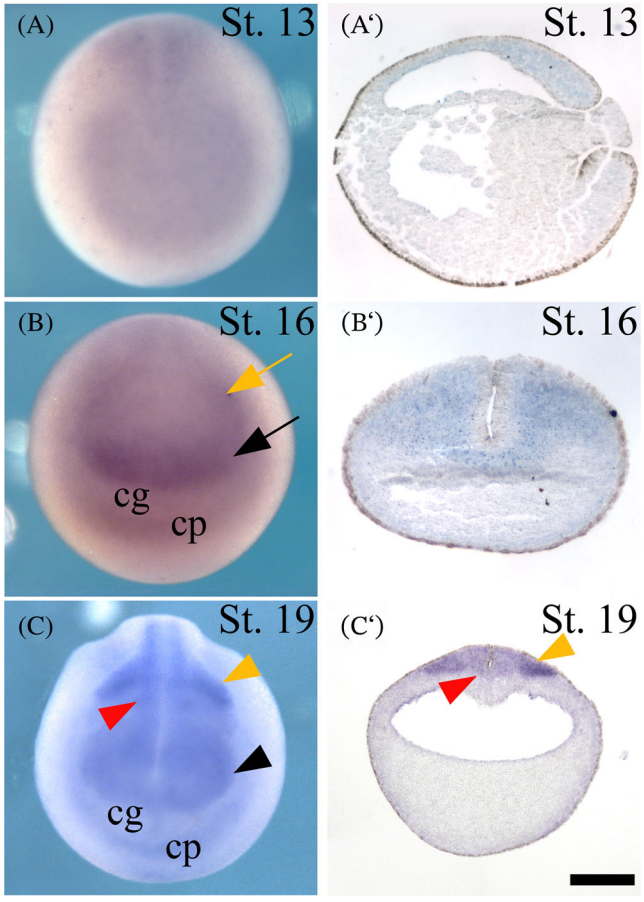

FIGURE 3 In situ hybridization analysis of *kdm7a* during neurulation. Embryo developmental stages are indicated at the top-right corner of each panel (St.: stage). Whole-mount embryos (A, B, C; frontal view, dorsal to the top) and respective sagittal (A′; frontal side to the left and dorsal side to the top) and transverse (B′, C′; dorsal side to the top) sections from whole-mount-stained embryos are represented in the panel. Black arrow indicates the anterior neural plate. Yellow arrow indicates neural crests. Red arrowheads indicate the neural tube. Black arrowhead indicates the optic vesicles. Yellow arrowheads indicate migrating neural crest cells. An average of 25 embryos was used for each of the analyzed stages. Scale bar: 300 μm. cg, cement gland; cp, cardiac progenitors.

During later stages of development (early tail bud, St. 25, Figure 4A,A′), *kdm7a* expression is observed in developing brain, eye vesicles, and branchial arches, which are all structures deriving from territories displaying *kdm7a* expression at neurula stage. In addition, new expression sites become clearly evident in the posterior region of the trunk, including the posterior wall and, more weakly, the proctodeum. A similar expression pattern is essentially maintained at later tail bud stages. At tail bud St. 32 (Figure 4B/B′,C–G), in particular, it is possible to recognize *kdm7a* expression in the prosencephalon, mesencephalon, and rhombencephalon, as well as in the retina, lens, and branchial arches. A distinct ISH signal is also observed in otic vesicles and in some cranial placodes, including lateral line, olfactory, and epibranchial placodes. At this stage, a weak signal appears at the level of pronephros as well. Finally, *kdm7a* mRNA expression strongly increases in the terminal region of the trunk, in particular at the level of the growing tail and proctodeum. In line with our results, ISH signals of *kdm7a* and *kdm7b* in post-somitogenesis zebrafish resulted prominent in the tectum, hindbrain, fin buds, and gills, and also distinguishable in the tail bud, suggesting evolutionarily conserved roles for this demethylase in vertebrate development.[6]

At St. 42 (Figure 5), *kdm7a* expression localizes in the prosencephalon, mesencephalon, and rhombencephalon (Figure 5A–C, respectively). In anterior regions, ISH signal is also observed in the olfactory pits and Jacobson's organ (Figure 5A). Additionally, *kdm7a* results transcriptionally activated in the velar plate, in the infrarostral cartilage, in cranial muscles including mandibular muscles, as well as in external ocular muscles, otic vesicles, and territories surrounding the internal gills (Figure 5B,C). In the trunk region, the expression is observed in the spinal cord and intestine (Figure 5D). Moreover, at St. 42, when neural retina development is assumed to be complete in *Xenopus*, *kdm7a* transcripts localize in the ONL, INL, and GCL, as well as in the plexiform layers (OPL, IPL) and ciliary marginal zone (CMZ) (Figure 5B,B′). In line with our data, other KDMs critically involved in retinal development are localized in the retina of adult rodents.[17,19,20] Finally, *kdm7a* ISH signal is observed in the outer regions of the lens.

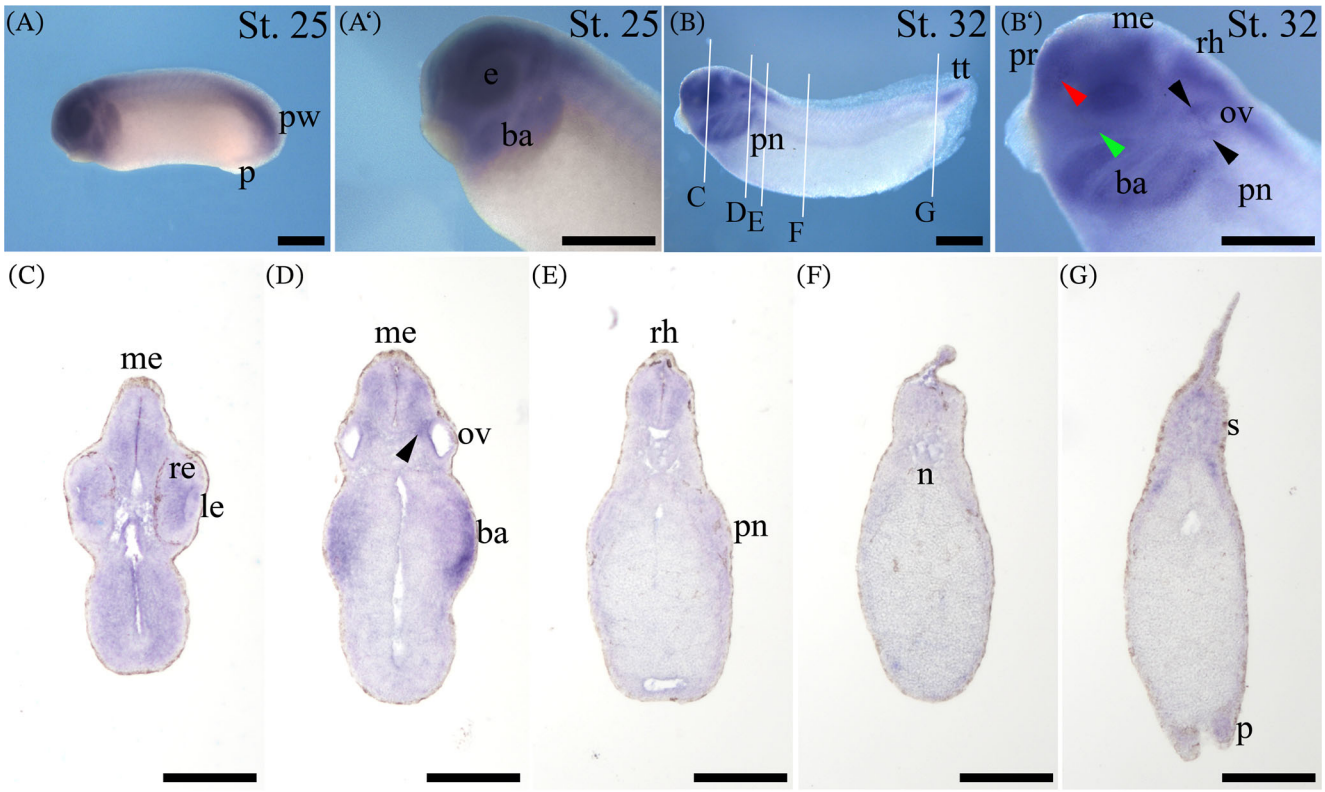

FIGURE 4 In situ hybridization analysis of *kdm7a* in tail bud embryos. Embryo developmental stages are indicated at the top-right corner of each panel (St.: stage). Lateral views of whole-mount hybridized embryos, anterior to the left (A, B). (A′, B′) magnified views of (A, B), respectively. White lines in (B) indicate the section planes shown in (C–G). Transverse sections from whole-mount St. 32 embryos, dorsal to the top (C–G). Black arrowheads indicate lateral line placode, red arrowhead indicates epibranchial placode, and green arrowhead indicates olfactory placode. An average of 25 embryos was used for each of the analyzed stages. Scale bar in (A–G, A′, B′): 500 μm. ba, branchial arches; e, eye; le, lens; me, mesencephalon; n, notochord; ov, otic vesicle; p, proctodeum; pn, pronephros; pr, prosencephalon; pw, posterior wall; re, retina; rh, rhombencephalon; s, somites; tt, tail tip.

2.3 | Gain of function experiments to address the role of *kdm7a* in retinogenesis

As *kdm7a* was previously highlighted in a screening aimed at selecting genes regulated by Rax/Rx1,[12] one of the master regulators of retina development, we addressed its potential role in two crucial phases of retinal cell-fate determination, that is, eye-field specification and late retinogenesis. To perform functional analyses, we focused on *kdm7a* gain-of-function (GoF) experiments (using *β-galactosidase* or *gfp* mRNAs as tracers), because the microinjection of morpholino antisense oligonucleotides targeting *kdm7a*, commonly used as a loss-of-function approach, turned out to be highly toxic for early embryos even at minimal doses (data not shown). Interestingly, analogous observations were reported for siRNA-mediated *kdm7a* knockdown in porcine embryos, which leads to cell death and severe reduction in the survival rate of blastocysts.[8] Such effects, observed using two different knockdown methodologies in two distinct models, suggest a potential important requirement for *kdm7a* in the early phases of the vertebrate embryonic development.

2.4 | Early markers of neural development are unaffected by *kdm7a* overexpression

To assess the function of *kdm7a* at early neurula stage, when the eye field is initially specified, we examined the effects of *kdm7a* overexpression on selected marker genes, which are in some cases determinants of distinct cell fates observable in the developing neural plate. In particular, we looked at *sox2*, expressed in neuronal precursors and involved in their maintenance,[27] *zic2*, and *zic3*, both expressed in the anterior neural plate and in neural crests,[28] as well as *rx1* and *cyclin d1*, regulators of early retinal fate and anterior neural plate proliferation, respectively,[12,29,30] and *n-tubulin*, a marker of differentiating neurons.[31] As shown in Figure 6, the microinjection of *kdm7a* mRNA did not significantly affect the expression of any of the analyzed genes, suggesting that *kdm7a* GoF in *Xenopus* is not sufficient to modulate early cell fate and neuronal differentiation in the neural plate, including the eye field.

Our results possibly misalign with previous findings indicating that in chick embryos and murine embryonic

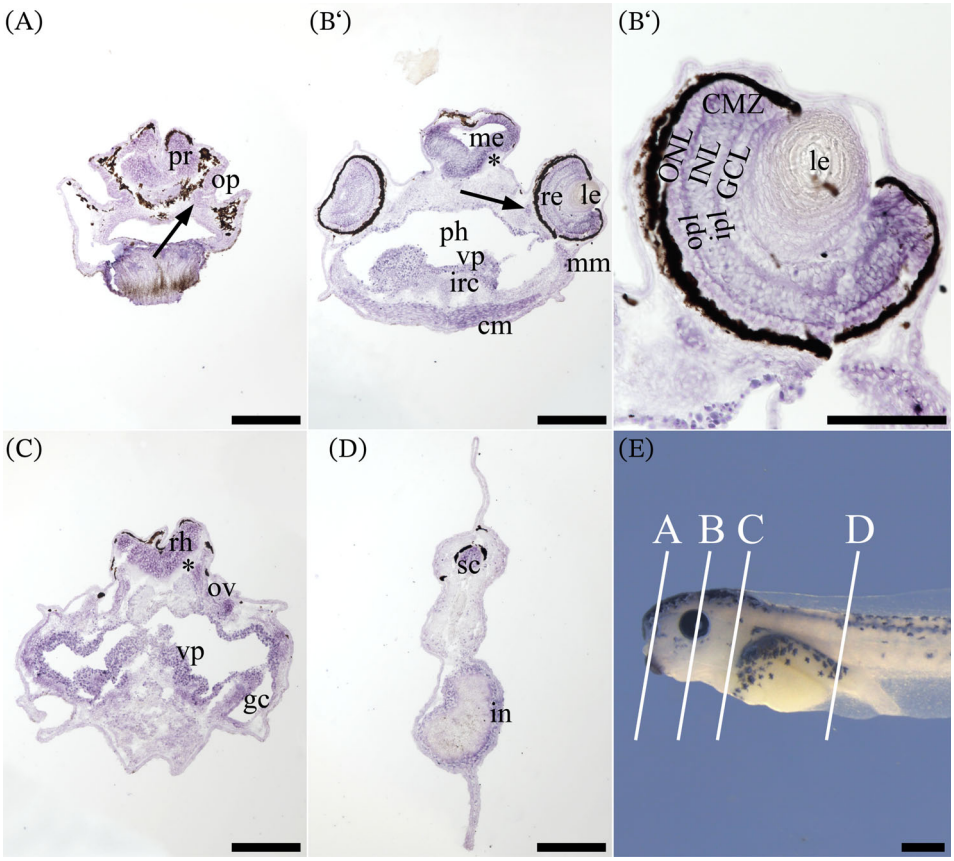

FIGURE 5 In situ hybridization analysis of *kdm7a* on stage 42 larvae cryosections. Transverse sections, dorsal side to the top (A, B, B′, C, D). Lateral views of the larvae, anterior side to the left (E). White lines in (E) indicate the section planes shown in (A, B, B′, C, D). Black arrows indicate the Jacobson's organ in (A) and the external ocular muscles in (B). (B′) high magnification of the eye represented in (B). Asterisk in (B) and (C) indicate the absence of hybridization signal at the level of the gray matter. For this analysis 10 embryos were used. Scale bars: 200 μm in (A, B, C, D); 500 μm in (E); 100 μm in (B′). cm, cranial muscles; CMZ, ciliary marginal zone; gc, gill chamber; GCL, ganglion cell layer; in, intestine; INL, inner nuclear layer; ipl, inner plexiform layer; irc, infrarostral cartilage; le, lens; me, mesencephalon; mm, mandibular muscles; ONL, outer nuclear layer; op, olfactory pit; opl, outer plexiform layer; ov, otic vesicle; ph, pharynx; pr, prosencephalon; re, retina; rh, rhombencephalon; sc, spinal cord; vp, velar plate.

stem cells *KDM7A* promotes neural cell fate.[4,9] These differences may reflect non-completely overlapping molecular mechanisms used in amniotes and anamniotes to achieve neural induction.[32]

2.5 | Effects of *kdm7a* overexpression on late retinal development

To explore the role of Kdm7a during late stages of retinal development, we evaluated the impact of *kdm7a* GoF on the reciprocal distribution of the major retinal neuronal populations in the mature retina (St. 42). As retinas were often very dense with GFP-positive (GFP+) cells, and therefore it was not possible to obtain a reliable count of their number, we quantified the reciprocal distribution of retinal neurons in terms of an "area index," expressed as the ratio between the area of a specific neural subpopulation and the overall area of the clones measured throughout the cryosectioned retina (see methods for details). As shown in Figure 7, compared to controls, in embryos subjected to *kdm7a* overexpression, ganglion cells are significantly reduced (about 15.5% reduction, $*p < .05$); horizontal cells are increased (about 206% increase, $*p < .05$), whereas the other retinal neural populations appear to be unaffected, indicating that *kdm7a* GoF influences the quantitative distribution of retinal neural subtypes. As area measurement depends on the number of cells as well as on their morphology, we cannot discriminate whether such differences are due to effects on proliferation or to changes of cell morphology. Further targeted studies aimed to explore this issue may be useful in the future. However, the reduced development of early retinal neuronal subtypes (ganglion cells), accompanied by an increased development of late retinal subpopulations (horizontal cells),[14] is suggestive of an alteration in the ordered generation of retinal cells through an impairment of the machinery regulating

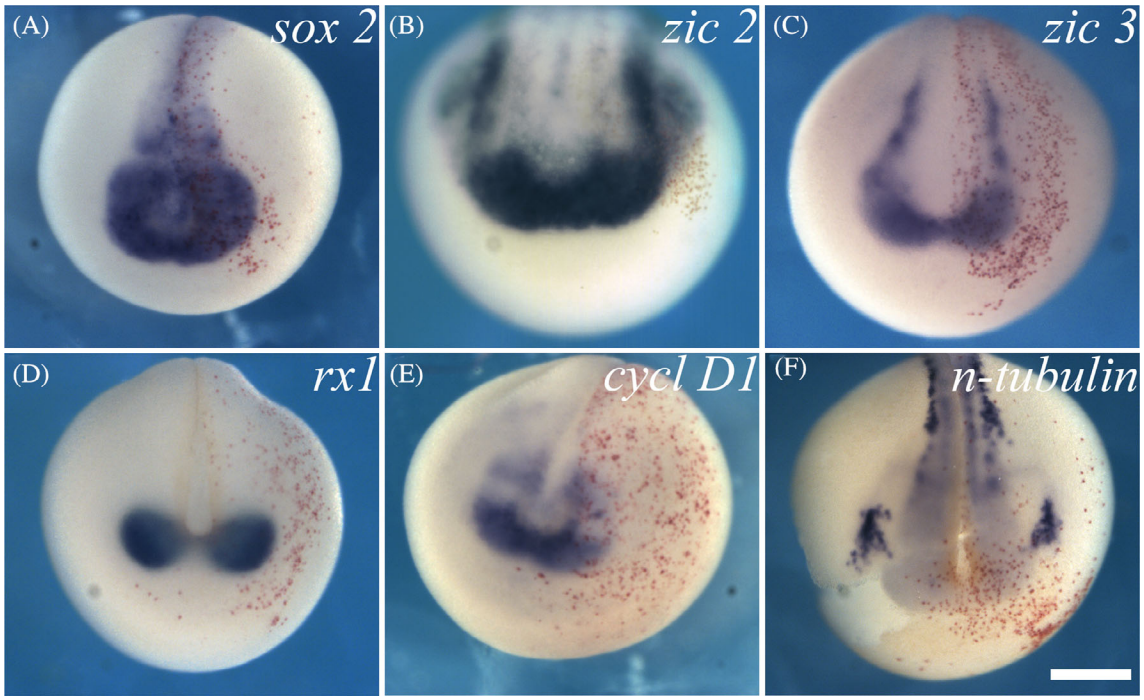

FIGURE 6 Whole-mount in situ hybridization analysis of neural plate markers. Frontal view (dorsal side to the top) of St. 13–16 embryos. The side of the embryos microinjected with *kdm7a* mRNA, together with nuclear *β-galactosidase* mRNA as a tracer (red spots), is on the right of each panel. The markers analyzed are indicated at the top-right corner of each panel. Images are representative of the phenotypes observed in 57/62 (A), 48/51 (B), 61/67 (C), 56/62 (D), 50/56 (E), and 48/52 (F) embryos analyzed, the remaining embryos displayed minor variations of the expression pattern. Scale bar: 300 μm.

retinal cell fate and/or RPCs cell-cycle exit and differentiation. In this respect, previous works in non-retinal cells of distinct experimental models suggested that KDM7A may be central in the regulation of these processes.[4,8,10,26] In addition, it has recently been indicated that conditional loss of some histone-specific methyltransferases may influence the transition from early to late competence of progenitor cells in the mouse retina, resulting in an abnormal production of retinal neural populations.[22] Additionally, it cannot be ruled out that the abnormal quantitative distribution we report may underlie an altered cell maintenance.

The lack of effects for *kdm7a* overexpression on neural plate markers appears unlikely to be due to inefficiency of the injected RNA, as the same *kdm7a* RNA affects late retinogenesis, occurring many hours later, in a cell type-specific manner. Therefore, different effects of *kdm7a* overexpression observed at distinct developmental times may rather reflect different competence of early neuronal precursors and retinal progenitors to respond to increased doses of *kdm7a* RNA. Nonetheless, this issue will be better investigated when an antibody reliably recognizing the *Xenopus* Kdm7a protein will be available, as well as in future studies aimed at addressing the histone methylation states. Notably, the influence of *kdm7a* overexpression on late retinogenesis is in agreement with a previous study in zebrafish, which indicated an important role for *kdm7a* orthologues mainly in late CNS development.[6]

Although, to our knowledge, this is the first study focusing on the functional role of *kdm7a* in retinal development, our results are in line with the general view emerging from previous reports, which indicate a pivotal role of histone demethylases for the formation of the retina in various experimental models. Coherently, these epigenetic regulators have been shown to influence, in a time-dependent manner, not only progenitors' proliferation and cell-fate determination, but also the maturation and apoptosis of specific subsets of retinal cells.[16–21]

3 | CONCLUSIONS

Our expression study provides novel notions expanding the current knowledge on the dynamic expression pattern of *kdm7a* in vertebrates. Furthermore, our functional analysis provides first evidence that *kdm7a* overexpression in *Xenopus* does not alter the early phases of retinal development, while affecting ganglion cells and horizontal cells formation during retinogenesis. Future

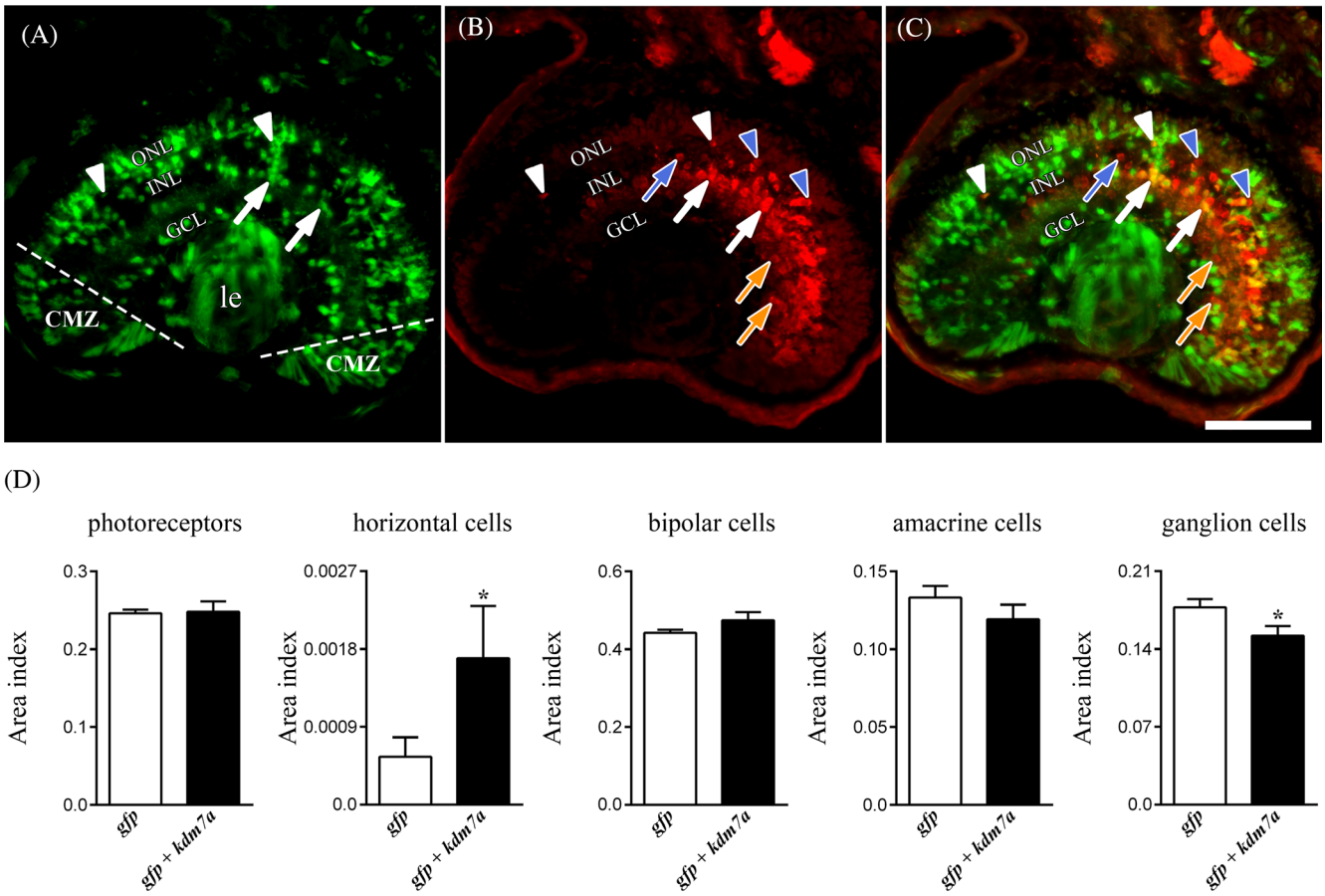

FIGURE 7 Evaluation of the relative area distribution of neuronal cells subtypes in mature retina. Representative images from cryosections of St. 42 tadpoles, showing GFP+ retinal clones (A, green), immunofluorescent horizontal and amacrine/displaced amacrine cells (B, red), and merge (C). White and blue arrowheads indicate examples of horizontal cells, notoriously localized in the outermost part of the INL (white: GFP+; blue: GFP−). White and blue arrows in the INL indicate examples of amacrine cells (white: GFP+; blue: GFP−). Orange arrows in the GCL indicate some displaced amacrine cells (all GFP- in this section). GFP+ cells of the clone that did not show immunofluorescence were unequivocally considered photoreceptors, ganglion cells, or bipolar cells, based on their location in the ONL, GCL, and INL, respectively, and based on their morphology. Scale bar (A, B, and C): 50 μm. (D) Quantitative analysis of relative "area index" obtained from $n = 9$ (*gfp*) and $n = 12$ (*gfp* + *kdm7a*) retinas. Data are expressed as mean ± standard error of the mean. Unpaired Student's *t*-test: $*p < .05$ (ganglion cells); Mann–Whitney *U*-test: $*p < .05$ (horizontal cells). CMZ, ciliary marginal zone; GCL, ganglion cell layer; INL, inner nuclear layer; le, lens; ONL, outer nuclear layer.

experiments should address the requirement of *kdm7a* for *Xenopus* retinal development, as well as its interactions with other epigenetic regulators.

4 | EXPERIMENTAL PROCEDURES

4.1 | Institutional review board statement

The animal study protocol was approved by the Italian Ministry of Public Health and the local Ethical Committee of the University of Pisa (authorization n. 501/2021-PR), in conformity with the Directive 2010/63/EU.

4.2 | Embryos manipulations and ISH

Embryos of *Xenopus laevis* were generated and staged in line with published works.[24,33] Whole-mount ISH was performed as previously described,[29] and signal detection was performed using BM Purple substrate (Roche, Indianapolis, IN, USA). Whole-mount images were acquired using a Nikon SMZ18 stereomicroscope (Nikon Corporation, Minato, TO, Japan), connected to a Nikon DS-Fi3 digital camera and equipped with the software NIS-Elements AR 5.11.03. The antisense probe for *kdm7a* was transcribed from the cDNA clone XL043i05 (GenBank Acc. n. BJ053034), by plasmid linearization with EcoRI followed by T7 RNA polymerase (Roche) in vitro transcription. In some cases, using a microtome,

20 μm-thick sections from whole-mount preparations were collected onto slides, and mounted with Eukitt (O. Kindler, Freiburg, Germany). Additionally, St. 42 tadpoles were fixed for 1 h in 4% paraformaldehyde (PFA) at room-temperature (RT), cryoprotected in 25% sucrose in phosphate buffer saline (PBS) overnight, sectioned using a cryostat (12 μm-thick sections), collected onto polarized slides, subjected to ISH in line with published methods,[34] and finally mounted with Aqua-Polymount (cat. No. 18606, Polysciences Inc., Warrington, PA, USA). ISH images obtained from tissue sections were captured by the microscope Nikon Eclipse Ti, connected to a Nikon DS-Fi3 digital camera and equipped with the software NIS-Elements AR 5.11.03.

4.3 | Microinjection

To generate a construct suitable for the transcription of injectable *kdm7a* mRNA, we inserted the full coding sequence, contained in the cDNA clone XL043i05, into a ClaI-XbaI-linearised pCS2+ plasmid. For GoF experiments, in line with published procedures,[12] *kdm7a* 5′-capped mRNA was injected in a volume of 4.6 nL, either in one dorsal blastomeres of four-cell stage embryos (500 pg) or in the animal dorsal blastomere D1.2 at 16-cell stage (150 pg). As lineage tracers, depending on the type of experiment, either nuclear *β-galactosidase* 5′-capped mRNA (300 pg) was coinjected in one dorsal blastomeres of four-cell stage, or *gfp* 5′-capped mRNA (100 pg) was coinjected in blastomere D1.2. Capped mRNAs used in this work were synthesized using the mMESSAGE mMACHINE SP6 Transcription Kit (cat. No. 1340 Ambion Incorporated, Austin, TX, USA), following manufacturer's instructions.

4.4 | Total RNA extraction and RT-qPCR

For each biological sample, total RNA was extracted from a pool of six to ten embryos, using TRIZOL reagent (Invitrogen, Carlsbad, CA, USA). Phenol-chloroform precipitation was performed to separate DNA and protein fraction from RNA. Then, RNA was precipitated and purified using RNAeasy Plus MiniKit (Qiagen, Venlo, The Netherlands), in line with manufacturer's instructions. Concentration and purity of total RNA were measured by DeNovix™ (Wilmington, DE, USA), while RNA integrity was evaluated by agarose-gel electrophoresis. First-strand cDNA was synthesized using QuantiTect Reverse Transcription Kit (Qiagen), according to manufacturer's instructions.

RT-qPCR, using the SYBR Green method (SensiMix SYBR kit, Bioline, London, UK) on a Rotor-Gene 6000 (Qiagen), was performed to evaluate mRNA levels, following the manufacturer's protocol. Expression level of *kdm7a* was normalized on the expression of three reference genes (*sub1.S*, *slc35b1.L*, and *ppp1ca.L*), in line with a previously described method,[35,36] and calculated as $2^{-(\Delta CT)}$. Primer-pair efficiency and specificity were evaluated before RT-qPCR experiments. To exclude genomic DNA contamination, negative controls obtained without reverse transcriptase were used. The following gene-specific sets of primers were used:

1. *kdm7a*: Fw 5′-ATTCTCCGACACCAAGATGG-3′, Rv 5′-TCATCGGGCCAGTAGTTTTC-3′;
2. *sub1.S*: Fw 5′-GCAGGAGAAATGAAGCCAGG-3′, Rv 5′-CCGACATCTGCTCCTTCAGT-3′;
3. *slc35b1.L*: Fw 5′-CGCATTTCCAAACAGGCTCC-3′, Rv-5′-CAAGAAGTCCCAGAGCTCGC-3′;
4. *ppp1ca.L*: Fw 5′-ACGAGTCTCTCATGTGCTCC-3′, Rv-5′-CAGAGCTGGGAGGGGTCATT-3′.

4.5 | Immunofluorescence and quantitative analysis

To evaluate the effects on quantitative distribution of the neural cell subpopulations in mature retina (St. 42) in terms of relative area, immunofluorescence on control animals and those subjected to *kdm7a* GoF was performed.

In preliminary experiments, aimed at selecting a limited number of antibodies necessary to investigate changes of relative area distribution among the major retinal neuron types, we evaluated the weight of Müller glia cells in this kind of quantification in the INL. In this respect, Müller cells were recognized by their morphology, and proved to be extremely rare in the GFP+ clones of either control specimens, in line with previous works in *Xenopus*,[37,38] or animals subjected to *kdm7a* overexpression, namely with no substantial differences among the two experimental conditions. Therefore, we considered that the contribution of Müller cells in terms of area in retinal clones was negligible and, for simplicity, we assumed that the area of the GFP+ cells in the INL not recognized by specific antibodies for horizontal and amacrine cells was attributable to bipolar cells.

Successively, for immunofluorescence analysis, cryosections (12 μm-thick) were incubated in a mixture containing both a rabbit polyclonal anti-GABA (ID# AB_572234; cat. No. 20094, Immunostar, Hudson, WI, USA) and a mouse monoclonal anti-TH (ID# AB_572268; cat. No. 22941, Immunostar) primary antibodies, both diluted 1:500 in 0.3% Triton X-100 (Sigma-Aldrich, Saint Louis, MO, USA) in PBS. Primary antibodies used in this study had been previously validated in *Xenopus laevis*.[39]

After washes, sections were incubated in a solution containing both Alexa Fluor 594 anti-rabbit (cat. No. A11037, Invitrogen) and Alexa Fluor 594 anti-mouse (cat. No. A11032, Invitrogen) secondary antibodies, both diluted 1:500 in 0.3% Triton X-100 (Sigma) in PBS, to reveal the immunolabeling in red. In this manner, among the GFP+ cells, it has been possible to simultaneously label the vast majority of amacrine-cell subpopulations, including the displaced amacrine cells, and the horizontal cells. To facilitate the recognition of the retinal layers, cell nuclei were successively counterstained with 300 ng/mL Hoechst 33258 (cat. No. 861405, Sigma) (data not shown). Finally, slides were mounted with Aqua-Polymount. Fluorescence images were acquired with the Nikon Eclipse Ti microscope.

GFP+ photoreceptors and GFP+ ganglion cells were easily recognized based on their unequivocal localization in the ONL and GCL, respectively. Similarly, immunofluorescent horizontal GFP+ cells and immunofluorescent amacrine GFP+ cells in the INL were discriminated from each other based on their typical spatial distribution, near the outer plexiform layer (OPL) and inner plexiform layer (IPL), respectively. Finally, non-immunolabeled GFP+ cells in the INL were considered bipolar cells. Using the software Adobe Photoshop CS 8.0.1 (Adobe Systems Inc., San Jose, CA, USA), green and red images were subjected to thresholding, to obtain the corresponding black-on-white images excluding the background, and by their combination the area of each retinal neural subpopulation was selected. For a given embryo, the area of a specific retinal subtype was measured in each section via the software ImageJ 1.48V (National Institutes of Health, Bethesda, MD, USA), and then summed to obtain a single total area. Finally, the ratio between this area and that deriving from the sum of the total areas of all cell subtypes of the same embryo was regarded as a relative "area index."

4.6 | Statistical analyses and image preparation

Statistics were performed using the software GraphPad Prism 6.0 (GraphPad Software, San Diego, CA, USA). After verification of the normal distribution, the appropriate test was applied. Differences were considered significant when $p < .05$.

All image panels presented in this work were prepared using the Adobe Photoshop CS 8.0.1 software.

ACKNOWLEDGMENTS

The authors are grateful to Naoto Ueno, for generously providing the plasmid XL043i05, and thank Salvatore Di Maria for frog care. This research was funded by intramural grants from University of Pisa to MA.

CONFLICT OF INTEREST STATEMENT

The authors declare no conflicts of interest. The funders had no role in the design of the study; in the collection, analyses, or interpretation of data; in the writing of the article; or in the decision to publish the results.

DATA AVAILABILITY STATEMENT

The datasets used and/or analyzed during the current study are available from the corresponding author on reasonable request.

ORCID

Massimiliano Andreazzoli https://orcid.org/0000-0001-9633-204X

REFERENCES

1. Delcuve GP, Rastegar M, Davie JR. Epigenetic control. *J Cell Physiol*. 2009;219(2):243-250. doi:10.1002/jcp.21678
2. Eckersley-Maslin MA, Alda-Catalinas C, Reik W. Dynamics of the epigenetic landscape during the maternal-to-zygotic transition. *Nat Rev Mol Cell Biol*. 2018;19(7):436-450. doi:10.1038/s41580-018-0008-z
3. Ganesan A, Arimondo PB, Rots MG, Jeronimo C, Berdasco M. The timeline of epigenetic drug discovery: from reality to dreams. *Clin Epigenetics*. 2019;11(1):174. doi:10.1186/s13148-019-0776-0
4. Huang C, Xiang Y, Wang Y, et al. Dual-specificity histone demethylase KIAA1718 (KDM7A) regulates neural differentiation through FGF4. *Cell Res*. 2010;20(2):154-165. doi:10.1038/cr.2010.5
5. Yokoyama A, Okuno Y, Chikanishi T, et al. KIAA1718 is a histone demethylase that erases repressive histone methyl marks. *Genes Cells*. 2010;15(8):867-873. doi:10.1111/j.1365-2443.2010.01424.x
6. Tsukada Y, Ishitani T, Nakayama KI. KDM7 is a dual demethylase for histone H3 Lys 9 and Lys 27 and functions in brain development. *Genes Dev*. 2010;24(5):432-437. doi:10.1101/gad.1864410
7. Horton JR, Upadhyay AK, Qi HH, Zhang X, Shi Y, Cheng X. Enzymatic and structural insights for substrate specificity of a family of jumonji histone lysine demethylases. *Nat Struct Mol Biol*. 2010;17(1):38-43. doi:10.1038/nsmb.1753
8. Rissi VB, Glanzner WG, De Macedo MP, et al. The histone lysine demethylase KDM7A is required for normal development and first cell lineage specification in porcine embryos. *Epigenetics*. 2019;14(11):1088-1101. doi:10.1080/15592294.2019.1633864
9. Huang C, Chen J, Zhang T, et al. The dual histone demethylase KDM7A promotes neural induction in early chick embryos. *Dev Dyn*. 2010;239(12):3350-3357. doi:10.1002/dvdy.22465
10. Swaminathan J, Maegawa S, Shaik S, et al. Cross-talk between histone methyltransferases and demethylases regulate REST transcription during neurogenesis. *Front Oncol*. 2022;12:855167. doi:10.3389/fonc.2022.855167

11. Meng Z, Liu Y, Wang J, et al. Histone demethylase KDM7A is required for stem cell maintenance and apoptosis inhibition in breast cancer. *J Cell Physiol*. 2020;235(2):932-943. doi:10.1002/jcp.29008
12. Giudetti G, Giannaccini M, Biasci D, et al. Characterization of the Rx1-dependent transcriptome during early retinal development. *Dev Dyn*. 2014;243(10):1352-1361. doi:10.1002/dvdy.24145
13. Blackshaw S, Harpavat S, Trimarchi J, et al. Genomic analysis of mouse retinal development. *PLoS Biol*. 2004;2(9):E247. doi:10.1371/journal.pbio.0020247
14. Andreazzoli M. Molecular regulation of vertebrate retina cell fate. *Birth Defects Res C Embryo Today*. 2009;87(3):284-295. doi:10.1002/bdrc.20161
15. Shin JY, Son J, Kim WS, Gwak J, Ju BG. Jmjd6a regulates GSK3beta RNA splicing in *Xenopus laevis* eye development. *PloS One*. 2019;14(7):e0219800. doi:10.1371/journal.pone.0219800
16. Watanabe S, Murakami A. Regulation of retinal development via the epigenetic modification of histone H3. *Adv Exp Med Biol*. 2016;854:635-641. doi:10.1007/978-3-319-17121-0_84
17. Umutoni D, Iwagawa T, Baba Y, et al. H3K27me3 demethylase UTX regulates the differentiation of a subset of bipolar cells in the mouse retina. *Genes Cells*. 2020;25(6):402-412. doi:10.1111/gtc.12767
18. Aldiri I, Moore KB, Hutcheson DA, Zhang J, Vetter ML. Polycomb repressive complex PRC2 regulates *Xenopus* retina development downstream of Wnt/beta-catenin signaling. *Development*. 2013;140(14):2867-2878. doi:10.1242/dev.088096
19. Raeisossadati R, Movio MI, Walter LT, Takada SH, Del Debbio CB, Kihara AH. Small molecule GSK-J1 affects differentiation of specific neuronal subtypes in developing rat retina. *Mol Neurobiol*. 2019;56(3):1972-1983. doi:10.1007/s12035-018-1197-3
20. Iida A, Iwagawa T, Kuribayashi H, et al. Histone demethylase Jmjd3 is required for the development of subsets of retinal bipolar cells. *Proc Natl Acad Sci U S A*. 2014;111(10):3751-3756. doi:10.1073/pnas.1311480111
21. Katoh K, Yamazaki R, Onishi A, Sanuki R, Furukawa T. G9a histone methyltransferase activity in retinal progenitors is essential for proper differentiation and survival of mouse retinal cells. *J Neurosci*. 2012;32(49):17658-17670. doi:10.1523/JNEUROSCI.1869-12.2012
22. Zhang J, Roberts JM, Chang F, Schwakopf J, Vetter ML. Jarid2 promotes temporal progression of retinal progenitors via repression of Foxp1. *Cell Rep*. 2023;42(4):112416. doi:10.1016/j.celrep.2023.112416
23. Schneider TD, Arteaga-Salas JM, Mentele E, et al. Stage-specific histone modification profiles reveal global transitions in the *Xenopus* embryonic epigenome. *PLoS One*. 2011;6(7):e22548. doi:10.1371/journal.pone.0022548
24. Newport J, Kirschner M. A major developmental transition in early *Xenopus* embryos: II. Control of the onset of transcription. *Cell*. 1982;30(3):687-696. doi:10.1016/0092-8674(82)90273-2
25. Glanzner WG, Rissi VB, de Macedo MP, et al. Histone 3 lysine 4, 9, and 27 demethylases expression profile in fertilized and cloned bovine and porcine embryos. *Biol Reprod*. 2018;98(6):742-751. doi:10.1093/biolre/ioy054
26. Yang X, Wang G, Wang Y, et al. Histone demethylase KDM7A reciprocally regulates adipogenic and osteogenic differentiation via regulation of C/EBPalpha and canonical Wnt signaling. *J Cell Mol Med*. 2019;23(3):2149-2162. doi:10.1111/jcmm.14126
27. Sasai Y. Roles of Sox factors in neural determination: conserved signaling in evolution? *Int J Dev Biol*. 2001;45(1):321-326.
28. Nakata K, Nagai T, Aruga J, Mikoshiba K. *Xenopus* Zic family and its role in neural and neural crest development. *Mech Dev*. 1998;75(1–2):43-51. doi:10.1016/s0925-4773(98)00073-2
29. Giannaccini M, Giudetti G, Biasci D, et al. Brief report: Rx1 defines retinal precursor identity by repressing alternative fates through the activation of TLE2 and Hes4. *Stem Cells*. 2013;31(12):2842-2847. doi:10.1002/stem.1530
30. Vernon AE, Philpott A. The developmental expression of cell cycle regulators in *Xenopus laevis*. *Gene Expr Patterns*. 2003;3(2):179-192. doi:10.1016/s1567-133x(03)00006-1
31. Chitnis A, Henrique D, Lewis J, Ish-Horowicz D, Kintner C. Primary neurogenesis in *Xenopus* embryos regulated by a homologue of the *Drosophila* neurogenic gene delta. *Nature*. 1995;375(6534):761-766. doi:10.1038/375761a0
32. Wilson SI, Edlund T. Neural induction: toward a unifying mechanism. *Nat Neurosci*. 2001;4:1161-1168. https://doi.org10.1038/nn747
33. Messina A, Lan L, Incitti T, et al. Noggin-mediated retinal induction reveals a novel interplay between bone morphogenetic protein inhibition, transforming growth factor beta, and sonic hedgehog signaling. *Stem Cells*. 2015;33(8):2496-2508. https://doi.org10.1002/stem.2043
34. D'Autilia S, Broccoli V, Barsacchi G, Andreazzoli M. *Xenopus* Bsx links daily cell cycle rhythms and pineal photoreceptor fate. *Proc Natl Acad Sci U S A*. 2010;107(14):6352-6357. doi:10.1073/pnas.1000854107
35. Vandesompele J, De Preter K, Pattyn F, et al. Accurate normalization of real-time quantitative RT-PCR data by geometric averaging of multiple internal control genes. *Genome Biol*. 2002;3(7):RESEARCH0034. doi:10.1186/gb-2002-3-7-research0034
36. Mughal BB, Leemans M, Spirhanzlova P, Demeneix B, Fini JB. Reference gene identification and validation for quantitative real-time PCR studies in developing *Xenopus laevis*. *Sci Rep*. 2018;8(1):496. doi:10.1038/s41598-017-18684-1
37. Kanekar S, Perron M, Dorsky R, et al. Xath5 participates in a network of bHLH genes in the developing *Xenopus* retina. *Neuron*. 1997;19(5):981-994. doi:10.1016/s0896-6273(00)80391-8
38. Zuber ME, Perron M, Philpott A, Bang A, Harris WA. Giant eyes in *Xenopus laevis* by overexpression of XOptx2. *Cell*. 1999;98(3):341-352. doi:10.1016/s0092-8674(00)81963-7
39. Viczian AS, Solessio EC, Lyou Y, Zuber ME. Generation of functional eyes from pluripotent cells. *PLoS Biol*. 2009;7(8):e1000174. doi:10.1371/journal.pbio.1000174

How to cite this article: Martini D, Digregorio M, Voto IAP, et al. *Kdm7a* expression is spatiotemporally regulated in developing *Xenopus laevis* embryos, and its overexpression influences late retinal development. *Developmental Dynamics*. 2023;1-11. doi:10.1002/dvdy.670